
I. BARIAKHTAR,^{1,2} A. NAZARENKO^{1,3}

¹Institute of Magnetism, Nat. Acad. of Sci. of Ukraine
(36-b, Vernadsky Blvd., Kyiv 03142, Ukraine)

²Boston College, Department of Physics
(140, Commonwealth Avenue, Chestnut Hill, MA 02467, USA)

³Harvard University, IAM-HUIT
(1033, Massachusetts Avenue, Cambridge, MA 02138, USA)

A MODEL FOR $d_{x^2-y^2}$ SUPERCONDUCTIVITY IN THE STRONGLY CORRELATED FERMIONIC SYSTEM

PACS 74.20.Mn, 74.25.Ha

Based on the known phenomenology of high- T_c cuprates and the available numerical calculations of the $t-J$ model, a two-dimensional effective fermionic model with the nearest neighbor attraction is proposed. Numerical calculations suggest that the model has the $d_{x^2-y^2}$ superconductivity (SC) in the ground state at a low fermionic density. We argue that this model captures the important physics of the $d_{x^2-y^2}$ superconducting correlations found earlier in the $t-J$ model by the exact diagonalization approach. Within a self-consistent RPA diagrammatic study, the density and the coupling strength dependence of the critical temperature is calculated. We also investigate the influence of the impurities on our results and show that the suppression of the superconductivity is insignificant, when the retardation effects are accounted for as opposed to the Hartree-Fock approximation.

Key words: superconductivity, strongly correlated fermionic system, $t-J$ model, mean-field approximation.

The Hubbard model with an *attractive* on-site interaction has played an important role in the qualitative understanding of s -wave superconductors. Several interesting problems, like the crossover from the BCS regime to the region where Cooper pairs form a Bose condensate (BC) [1], can be addressed within this model, by using analytical and numerical techniques [2]. The more realistic microscopically derivable electron-phonon Hamiltonian is the underlying model for the attractive Hubbard one. Although the phononic degrees of freedom are not explicit, it is expected that the qualitative properties of the attractive Hubbard model are the same as those of the electron-phonon one, while the latter is much more difficult to study numerically or analytically.

However, since it has been conclusively established that the high critical temperature (high- T_c) super-

conductors have a condensate with pairs formed in the $d_{x^2-y^2}$ channel [3, 4], the direct relevance of the on-site attractive Hubbard model for cuprates is questionable. In addition, the studies of H_{c2} in cuprates suggest that the Cooper pairs are only several lattice spacings in size, locating the high- T_c materials in an intermediate region between the BCS and the BC limits [4]. In this regime, the BCS mean-field (MF) approximation is not quantitatively accurate [5]. Thus, it would be desirable to have a fermionic model with a $d_{x^2-y^2}$ superconducting ground state that can be studied with reliable non-perturbative diagrammatic and computational techniques in the small coherence length region. Results obtained in this framework could be directly compared with the cuprate phenomenology. The ideas presented in this research can be applied to the recently discovered iron-pnictide superconductors, which also exhibit the unconventional behavior having the pairing symmetry in the nodal

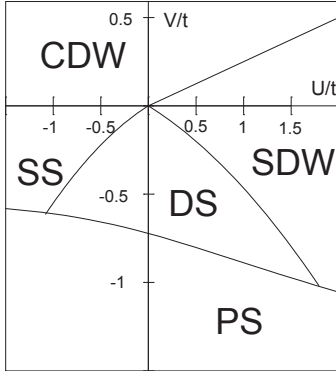


Fig. 1. Mean-field phase diagram of the $t - U - V$ model at half-filling [5]. DS, SS, PS, CDW, and SDW denote d -wave SC, s -wave SC, phase separation, charge-density-wave, and spin-density-wave order, respectively

d_{xy} -wave channel, and their phase diagram has regions, where the superconducting state emerges in the existing antiferromagnetic environment [6].

How can one construct a minimal model that can provide the generalization of the attractive Hubbard model to the case of $d_{x^2-y^2}$ superconductivity? The current literature shows that many studies of d -wave superconductors are performed, by using the BCS MF approximation after introducing a proper attractive kernel in the gap equation to induce d -wave correlations. This approach is accurate in a weak coupling, where pairs are large, but it does not address the regime of small pairs which is more realistic for cuprates. To improve these results, it is natural to consider, as a first candidate for a model with d -wave SC, the so-called $t - U - V$ model [7], where U is repulsive on-site, V is the strength of a density-density attraction at a distance of one lattice spacing a , and t is the amplitude of a nearest-neighbor (n.n.) hopping term. In the MF approximation [7], the phase diagram of the $t - U - V$ model at the half-filling (Fig. 1) has, indeed, an “island” of d -wave SC. However, it is worth to note the small size of this phase caused by the competition with the phase separation (PS), where electrons doubly occupy a macroscopic region of the cluster to minimize the energy. A recent study [8] has shown that the effect of PS cannot be simply avoided by introducing a long-range Coulomb repulsion, since PS may be replaced in this situation by a charge-density-wave (CDW) state, rather than by SC. Thus, the competition SC-PS is subtle and not created by the absence of long-range interactions [9].

The techniques beyond the MF approximation further show that the $t - U - V$ model is of very limited use for the study of d -wave superconductors. Analyzing the results obtained with the use of the Quantum Monte Carlo (QMC) and Exact Diagonalization (ED) techniques [10] at small U/t , where the MF approximation predicts a d -wave condensate, it becomes clear that the competition with PS occurs. This phase can be observed numerically with QMC simulations, since it was found in some regions of the parameter space that the mean particle density converges to two very different results depending on the randomly chosen initial Hubbard–Stratonovich fields. Such a behavior is typical of systems with two competing minima in the free energy, as it happens in the presence of PS.

Thus, it would be desirable to have a model free from the problems described above, where carriers at a *small* density form pairs, mimicking the expected hole-pairing of cuprates. The $t - U - V$ model at a low electronic density has s -wave SC rather than d -wave SC [7], by complicating matters further. An inescapable conclusion of this analysis is that it is necessary to go beyond the $t - U - V$ model for a proper study of effective fermionic models for d -wave SC [11]. It is remarkable that, in spite of the recent huge effort devoted to the study of d -wave SC in cuprates, the analog of the attractive Hubbard model for $d_{x^2-y^2}$ pairs still seems unknown.

The main purpose of this paper is to discuss a fermionic model for $d_{x^2-y^2}$ SC, which solves the problems found in the $t - U - V$ Hamiltonian. This topic embraces a huge effort by the condensed matter community and introduces a set of potential candidates [12]. Before the construction of such a phenomenological model, we start with identifying a higher level underlying model, which would be microscopically derivable, on the one hand, and, on the other hand, would have numerical results suggesting strong pairing correlations in the d -wave channel in the ground state. In the case of the attractive Hubbard model with the s -wave superconductivity, such higher-level model is the electron-phonon Hamiltonian. For the d -wave superconductivity, the best candidate for such starting point is, in our view, the $t - J$ model in the regime of low doping. Indeed, in the elaborate and sophisticated *ab initio* numerical study [13], the parameters of the $t - J$ model were mapped to the microscopic parameters of the multiband $p - d$ model,

which, in turn, is in direct relation to the microscopic chemical and crystal structure of cuprates. An independent significant numerical effort was devoted to studying the possible orders in the $t - J$ model. As a result, the clear indications of d -wave pairing correlations were found in the region of parameters relevant to cuprates [14]. However, the $t - J$ model itself is hard to be studied analytically or numerically, especially in the regime of low doping, which is, in fact, the most relevant to the physics of cuprates [10]. Thus, in order to better access this region with a wider variety of the techniques, in particular self-consistent diagrammatics, we attempt to go one level of simplification further and to construct a minimal phenomenological model specifically for the d -wave superconductivity with the parameters based on the accessible numerical results for the $t - J$ model.

Analyzing the model studied here with computational techniques shows that it presents strong pairing correlations in the d -wave channel (and PS does not cause serious problems) [14]. The Hamiltonian contains an attractive n.n. density-density interaction at the distance a , as in the $t - U - V$ model, but it differs from it in the fermionic dispersion, which is dominated in the new model by hopping within the *same* sublattice, i.e. linking next-nearest-neighbor (n.n.n.) sites (see Fig. 2, *a*). This model was discussed before in the context of the ‘‘Antiferromagnetic van Hove’’ (AFVH) scenario for the cuprates, where the high T_c is induced by a large peak in the hole density of states (DOS) caused by antiferromagnetism [15]. The intra-sublattice dispersion is natural if the holes move in a nearly antiferromagnetic background that is energetically costly to be disturbed. The attractive interaction has its origin in AF correlations. In [15], the model was studied only within the MF approximation. But here, we substantially improve the analysis using a computational self-consistent diagrammatic technique. The Hamiltonian of the proposed model as a candidate for d -wave SC is

$$H = \sum_{\mathbf{k}\alpha} \epsilon_{\text{AF}}(\mathbf{k}) \left[c_{\mathbf{k}\alpha}^\dagger c_{\mathbf{k}\alpha} + \text{h.c.} \right] - |V| \sum_{\langle ij \rangle} n_i n_j, \quad (1)$$

where $\alpha = A, B$ indicates the sublattice; $\epsilon_{\text{AF}}(\mathbf{k}) = 4t_{11} \cos k_x \cos k_y + 2t_{20}(\cos 2k_x + \cos 2k_y)$ is the dispersion; t_{11}, t_{20} , and V are parameters; and n_i is the number operator, with the rest of the notation to be standard. The operators c satisfy anticommutation relations. They do not have a spin index,

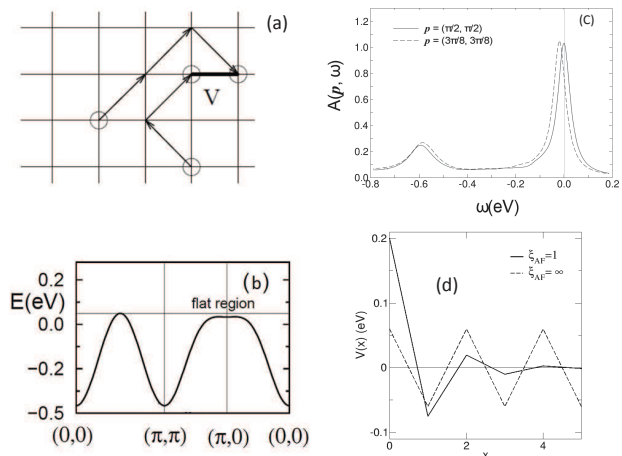


Fig. 2. (a) Schematic representation of model (1). Fermions move within the same sublattice, and interact at distance one; (b) the quasiparticle energy vs the momentum obtained at the half-filling with the use of the $t - t' - J$ model [16]. The result shown is a good fit of Monte Carlo data on a 12×12 cluster at $J/t = 0.4$; (c) Spectral weight $A(\mathbf{p}, \omega)$ for one hole in an antiferromagnet calculated using the rainbow approximation. The first excited state is the ‘‘string state’’ and is located at $\omega \sim -0.6$ eV; (d) $V(x)$ along the x -axis after the Fourier transformation of the smeared potential $V(\mathbf{p}) = \delta(\mathbf{p} - \mathbf{Q})$ (see the text); ξ_{AF} is given in lattice units

but carry a sublattice index which plays a similar role. Particles are distributed such that a half of them are in each sublattice. Intuitively, the particles described by Eq. (1) represent ‘‘holes’’ in the cuprates.

The origin of the hole dispersion in Eq.(1) (see Fig. 2, *b*) is the analytical fit to the numerically calculated positions of the quasiparticle maxima of the spectral function for different momenta within the framework of the $t - t' - J$ model (t' was added to the model to better fit the experimental results). Fig. 2, *c* demonstrates the spectral weight $A(\mathbf{p}, \omega)$ for one hole in an antiferromagnet calculated with the use of the rainbow approximation. Different numerical techniques produce very similar results [16], and all are in excellent agreement with the generalized tight-binding study and with the photoemission results for $\text{Sr}_2\text{CuO}_2\text{Cl}_2$ [13, 17]. This emphasizes a deep relation between the simple model under consideration, on the one hand, and the $t - J$ and the microscopic structure of the cuprates, on the other hand. To ensure that the one-particle dispersion is robust against an increase in the hole concentration, the further numerical study was undertaken, which showed that the quasiparti-

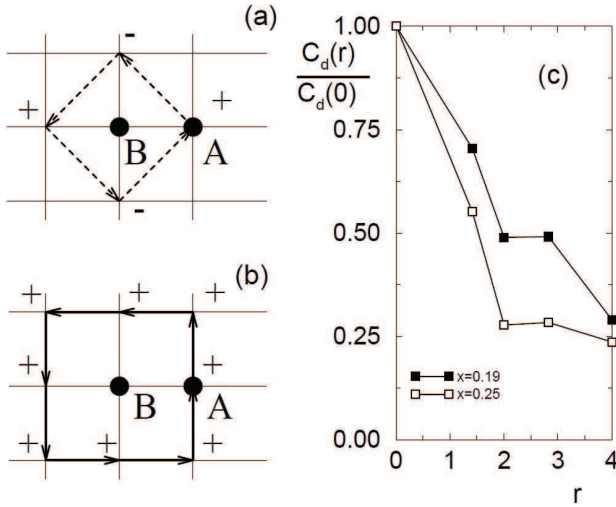


Fig. 3. Two fermions in the large $|V|$ limit of Eq. (1) showing the $d_{x^2-y^2}$ -wave character of the bound state (a); two fermions in the large $|V|$ limit of the $t-U-V$ model (b). The bound state is the s -wave; (c) $d_{x^2-y^2}$ pairing correlations vs the distance r for Eq. (1) at $T = 0$ studied with the exact diagonalization techniques on a 32-site cluster. The couplings are $|V|/t_{11} = 1.0$, $t_{20}/t_{11} = 0.4$, and x is indicated. Correlations in the s - and p -channels are negligible [14]

cle peak still carries a spectral weight up to the hole concentrations of about 25% [18]. Note that the numerically obtained dispersion in Fig. 2, *b* reflects the remarkable feature of the hole-doped cuprates near the optimal doping, namely the presence of a universal flat band dispersion near $(\pi, 0)$ [4] that cannot be explained using band structure calculations.

For the NN attraction between these quasiparticles, induced by a local AF phase fluctuation, it may seem questionable whether one can use the same interaction both at and away from the half-filling. However, the hole-hole potential is not much affected at distances shorter than ξ_{AF} . This can be illustrated by a real space analysis (Fig. 2, *d*) of a smeared δ -function potential of the AF origin $V(\mathbf{q}) = \xi_{AF} / [1 + \xi_{AF}^2(\mathbf{q} - \mathbf{Q})^2]$, where the lattice spacing is set to 1, and $\mathbf{Q} = (\pi, \pi)$. Figure 2, *d* shows that the NN potential ($x = 1$) does not change noticeably, as ξ_{AF} is reduced, while $V(x > 1)$ is rapidly suppressed. This simple analysis agrees surprisingly well with more sophisticated studies of the real space potentials in such systems (see, e.g., [19,20]) Then, using the same NN form of the potential for many densities should not be a bad approximation. Note that the lo-

cal character of the real-space potential does not imply small Cooper pairs. Their size can be regulated, by using both its range and intensity, even though small cluster calculations often underestimated the d -wave pair size [21].

What is the origin of the d -wave symmetry in the ground state of the two-body problem? Let us consider the large $|V|$ limit and analyze the movement of one particle around another one as schematically shown in Fig. 3, *a*. In this regime, the energy is minimized, when the interparticle distance is one lattice spacing at all times. Keeping particle B fixed at a given site, the problem now amounts to solving an effective four-site hopping Hamiltonian of particle A moving along the four n.n. sites to B using the hopping amplitude t_{11} along the diagonal. Here, it is important to observe that the sign of t_{11} is chosen as a *positive* number by the requirement that the minimum in the dispersion be at $\mathbf{p} = (\pi/2, \pi/2)$ or $(0, \pi)$, as it is natural in problems of holes in antiferromagnets [15]. The signs of t_{11} and t_{20} are physically relevant, unlike the sign of a n.n. hopping that can be changed by suitable transformations on a square lattice. Then, the ground state of the effective four-site problem corresponds to selecting a phase alternating in sign for particle A (Fig. 3, *a*). This leads to a $d_{x^2-y^2}$ bound state, providing a real-space intuitive explanation for the appearance of d -wave pairs, which complements those based on the perturbative interchange of magnons [3]. We remark that this simple result found in Eq.(1) is not present in the $t-U-V$ model. If the n.n.n. hopping (Fig. 3, *a*) is replaced by the n.n. hopping of the $t-U-V$ model, then the ground-state phases of particle A orbiting around B at large $|V|$ are as those shown in Fig. 3, *b*. They correspond to the s -wave bound state.

The presence of $d_{x^2-y^2}$ bound states in the two-body problem of Eq. (1) suggests SC in the same channel at a finite particle density. However, CDW and PS states are also favored by a particle-particle attraction. Thus, an explicit calculation is needed to verify the existence of a SC condensate. In the earlier numerical study of the ground-state pairing correlations $C_d(\mathbf{r})$ on a $\sqrt{32} \times \sqrt{32}$ site cluster with the use of exact diagonalization techniques, it was found that d -wave strong pairing correlations exist in the ground state of Hamiltonian (1) supplemented by mild higher order repulsion, unlike the results obtained before for the $t-U-V$ model [14].

Hamiltonian (1) can also be studied diagrammatically, by using Eliashberg-type equations [22]. With this approach, we have calculated T_c vs x in the intermediate to strong coupling region. Working in the Matsubara space and in natural units, we approximate the normal state proper self-energy, by iteratively solving the equation

$$\Sigma(\mathbf{k}, \omega_n) = -\frac{T}{N} \sum_{\mathbf{q}, \omega'_n} V_{\text{eff}}(\mathbf{k} - \mathbf{q}, \omega_n - \omega'_n) G(\mathbf{q}, \omega'_n), \quad (2)$$

where N is the number of sites (we used a 32×32 cluster for this calculation), T the temperature, $\omega_n = (2n + 1)\pi T$ ($-\infty < n < +\infty$), the full normal state one-particle Green's function satisfies $G(\mathbf{k}, \omega_n) = 1/[i\omega_n - (\epsilon_{\text{AF}}(\mathbf{k}) - \mu) - \Sigma(\mathbf{k}, \omega_n)]$, and $V_{\text{eff}}(\mathbf{k}, \omega_n)$ is the RPA effective potential with particle-hole bubbles containing G , rather than the non-interacting Green's function, to make the calculation self-consistent. Once the normal state G is found, we use

$$\Phi(\mathbf{k}, \omega_n) = \sum_{\mathbf{q}, \omega'_n} M(\mathbf{k}, \mathbf{q}, \omega_n, \omega'_n) \Phi(\mathbf{q}, \omega'_n) \quad (3)$$

for the SC state. Here, $\Phi(\mathbf{k}, \omega_n)$ is the anomalous self-energy, which can be considered as an order parameter for SC, and $M(\mathbf{k}, \mathbf{q}, \omega_n, \omega'_n) = -\frac{T}{N} V_{\text{eff}}(\mathbf{k} - \mathbf{q}, \omega_n - \omega'_n) G(\mathbf{q}, \omega'_n) G(-\mathbf{q}, -\omega'_n)$. We have solved Eqs. (2) and (3) self-consistently at different temperatures and densities, using ten times the bandwidth as an energy cutoff. The symmetry of the SC condensate is determined from the symmetry of the eigenvector of Eq. (3) corresponding to the largest eigenvalue [22]. After all ring diagrams are summed up [23], this symmetry is $d_{x^2-y^2}$.

The results for T_c are shown in Figs. 3 *a, b* compared to the MF approximation [15], which is equivalent in this model to the Hartree-Fock (HF) approximation. The qualitative agreement is good. Quantitatively, the self-consistent approach reduces T_c at the optimal doping by a factor ~ 1.5 still maintaining T_c at a high value (note that, at small concentrations, T_c tends to zero, but the small x region on the phase diagram of the cuprates is dominated by the AF order, and the superconductivity is suppressed). No drastic further reductions of T_c are expected by adding diagrams beyond RPA to the calculation. The reason is that, in this model, the vertex correction identically *vanishes* due to intrinsic fea-

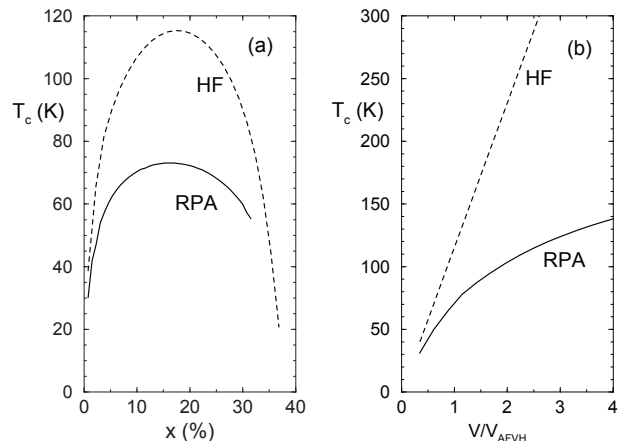


Fig. 4. (a) Critical temperature T_c of model (1) vs the fermionic density x , using $t_{11} = 0.165$ eV, $t_{20} = 0.0435$ eV, and $V = -0.075$ eV, as suggested by the high- T_c phenomenology [9]. The solid line corresponds to the self-consistent RPA approximation. The dashed line is the MF or HF result [9]; (b) T_c vs the coupling constant V , with t_{11}, t_{20} fixed as in (a), at the density where T_c is maximum in (a). V is in units of $V_{\text{AFVH}} = -0.075$ eV, the coupling used in [9]

tures of Hamiltonian (1) namely such that the particles move within the same sublattice, while the interaction is an intersublattice one. To understand this effect, we consider the real-space representation of the vertex correction contribution to the self-energy, which is given by $\Sigma^{\text{vertex}}(\mathbf{r}, \tau) \propto \sum_{\mathbf{e}_1, \mathbf{e}_2 = \hat{x}, \hat{y}} G(\mathbf{r} + \mathbf{e}_1, \tau) G(\mathbf{r} + \mathbf{e}_1 + \mathbf{e}_2, -\tau) G(\mathbf{r} + \mathbf{e}_2, \tau)$. It is clear that there is always Green's function that vanishes, irrespective of whether \mathbf{r} connects the same or different sublattices. Finally, we note that the values of T_c shown in Fig. 4, *a* are realistic, and the presence of an “optimal” density is a consequence of the peak in the DOS of $\epsilon_{\text{AF}}(\mathbf{k})$ [15].

Next, we will include the influence of the impurities in our study to address the small disorder influence on the properties of the d -wave condensate. This problem is long standing in the area of the correlated system, in general, and in the physics of the cuprates, in particular (see [24] and references therein). Our present study is concentrated on the influence of impurities on the critical temperature and the overall stability of the d -wave condensate at the introduction of a small disorder. We will treat impurities in the Born approximation and, in addition, consider them to be dilute and uncorrelated [25]. In this case, the scattering is *elastic*. Within this approximation,

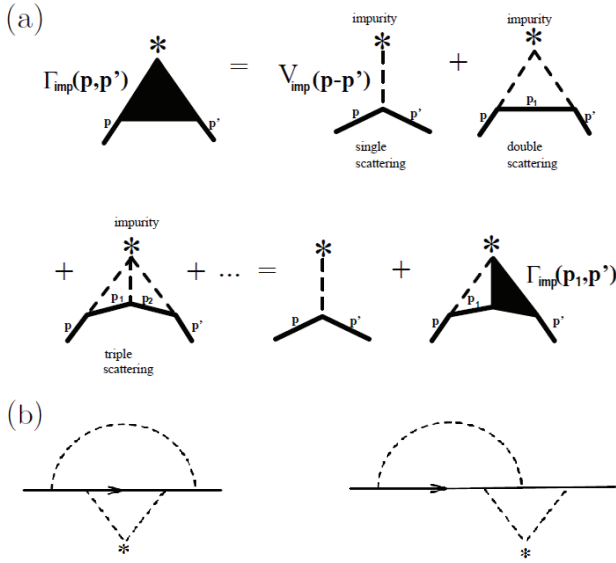


Fig. 5. (a) impurity vertex; (b) combination of impurity scattering and two-body potential processes (see the text)

one accounts, partially or fully, only for the set of diagrams depicted in Fig. 5, *a* as contributing to the irreducible self-energy. These diagrams are proportional to the impurity concentration n_i , while the others are of a higher order in n_i and, therefore, discarded (e.g., like those containing the potential lines that cross) [25]. This approximation is exact in the first order of the impurity concentration in the meaning that the positions of impurities are averaged. In the case of dense impurities, it is not correct, because the system is no longer uniform.

The diagrams, that are kept, represent an infinite set of the multiple Born scattering processes on the same impurity starting with the single scattering process. Figure 5, *a* shows the integral equation for the irreducible impurity vertex $\Gamma_{\text{imp}}(\mathbf{p}, \mathbf{p}', \omega_n)$ after the summation of the infinite series:

$$\Gamma_{\text{imp}}(\mathbf{p}, \mathbf{p}', \omega_n) = V_{\text{imp}}(\mathbf{p} - \mathbf{p}') + \frac{1}{N} \sum_{\mathbf{p}_1} V_{\text{imp}}(\mathbf{p} - \mathbf{p}_1) G(\mathbf{p}_1, \omega_n) \Gamma_{\text{imp}}(\mathbf{p}_1, \mathbf{p}', \omega_n),$$

where $V_{\text{imp}}(\mathbf{q})$ is the Fourier transform of the bare impurity potential, i.e. $V_{\text{imp}}(\mathbf{q}) = \sum_{\mathbf{x}} \exp(-i\mathbf{x} \cdot \mathbf{q}) \times V_{\text{imp}}(\mathbf{x})$ corresponding to the dashed line. Fermionic lines are not straight on the figure to indicate that the momentum changes its direction (but not the

absolute value) after each scattering. In vacuum, the impurity vertex is proportional to the full scattering amplitude $f(\mathbf{p}, \mathbf{p}')$ for a free particle of mass m and kinetic energy $\frac{p^2}{2m}$ scattered on a potential $V_{\text{imp}}(\mathbf{q})$: $\Gamma_{\text{imp}}(\mathbf{p}, \mathbf{p}', \omega_n) = -\frac{2\pi\hbar^2}{m} f(\mathbf{p}, \mathbf{p}')$. The proper self-energy addition due to the impurity scattering is

$$\Sigma_{\text{imp}}(\mathbf{p}, \omega_n) = n_i \Gamma(\mathbf{p}, \mathbf{p}, \omega_n),$$

where n_i is the concentration of impurities, and should be *added* to the two-body proper self-energy. This sum of two terms is to be substituted in the Dyson equation:

$$G(\mathbf{k}, \omega_n) = G_0(\mathbf{k}, \omega_n) + G_0(\mathbf{k}, \omega_n) [\Sigma(\mathbf{k}, \omega_n) + \Sigma_{\text{imp}}(\mathbf{k}, \omega_n)] G(\mathbf{k}, \omega_n).$$

To give a clear idea of diagrams included and excluded, the two typical diagrams are presented in Fig. 5, *b*. The first one is implicitly kept (note that the inner fermionic lines are thin): it is not compact, since the inner line is loaded with the impurity self-energy and, hence, does not explicitly contribute to the irreducible self-energy (if the lines were thick, it would lead to the double counting). But it will appear in the expansion when the thick line is substituted with the thin one and the self-energy. The second diagram is compact and excluded. It would contribute explicitly to the irreducible self-energy if it were included. Now, we consider the impurity potential, which is assumed *local* and spin-independent. Its Fourier transform is a momentum-independent constant U_{imp} . Then, directly applying the rules above, one can obtain the contribution from the m -fold scattering process to the proper self-energy, namely:

$$\begin{aligned} \Sigma_{\text{imp}}(\omega_n) &= \frac{n_i}{N^{m-1}} \times \\ &\times \sum_{\mathbf{p}_1 \dots \mathbf{p}_{m-1}} U_{\text{imp}} G(\mathbf{p}_1, \omega_n) U_{\text{imp}} \dots G(\mathbf{p}_{m-1}, \omega_n) U_{\text{imp}} = \\ &= \frac{n_i}{N^{m-1}} U_{\text{imp}}^m \left[\sum_{\mathbf{k}} G(\mathbf{k}, \omega_n) \right]^{m-1}. \end{aligned}$$

The first-order Born scattering ($m = 1$) is just the zero momentum Fourier component of the impurity potential times the impurity concentration $n_i U_{\text{imp}}$, which is just a constant to be absorbed by the chemical potential later on (as it happens to the tadpole

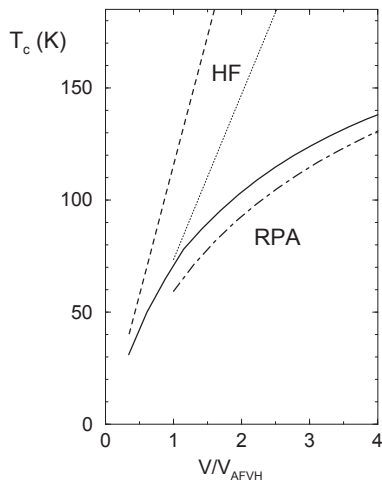


Fig. 6. Influence of dilute impurities on T_c : solid line is the result of pure RPA calculations, dot-dashed line is obtained in the “dirty” RPA; dashed line is the pure HF approximation, dotted line is the “dirty” HF case. Strong coupling calculation is much less affected by the impurities than the HF approximation

diagrams [26]). Thus, the minimal nontrivial account for the impurities is contained in the second-order Born term $\frac{n_i N^2}{U} \sum_{\mathbf{k}} G(\mathbf{k}, \omega_n)$ ($m = 2$), which is considered in the literature as the “weak scatterer limit”. Then one can calculate directly the *unitary* (or the strong scatterer) limit, when all the proper diagrams are summed up. The irreducible self-energy due to the multiple Born scattering to all orders is the infinitely descendant geometric series sum:

$$\Sigma_{\text{imp}}(\omega_n) = \frac{n_i \frac{U_{\text{imp}}^2}{N} \sum_{\mathbf{k}} G(\mathbf{k}, \omega_n)}{1 - \frac{U_{\text{imp}}}{N} \sum_{\mathbf{k}} G(\mathbf{k}, \omega_n)}.$$

Note that the impurity vertex is momentum-independent in this case:

$$\Gamma_{\text{imp}}(\mathbf{p}, \mathbf{p}', \omega_n) = \frac{U_{\text{imp}}}{1 - \frac{U_{\text{imp}}}{N} \sum_{\mathbf{k}} G(\mathbf{k}, \omega_n)}.$$

Figure 6 presents the influence of the multiple isotropic impurity scattering (unitary limit) on T_c : the result for a system with 10% impurities of the strength $U = 0.25$ eV is depicted to compare with that for the clean system. The dependence $T_c(V)$ is affected rather modestly (less than a 10%-drop in the RPA case) for such severe amount of “dirt”. One can see that, for 10% of impurity, the system is still a high temperature superconductor.

Summarizing, we have studied a model for fermions moving on a 2D square lattice with the intrasublattice hopping and attractive n.n. density-density interactions. Using numerical and analytical techniques, we conclude that, in this model, (i) the two-body problem leads to a $d_{x^2-y^2}$ -wave bound state in a natural way, and (ii) in the dilute limit, the ground state has strong $d_{x^2-y^2}$ pairing correlations. We have also provided the evidence of that the $t - U - V$ model actually does not show a clear signal of d -wave SC in computational studies, and the competition with PS prevents the analysis of its intermediate coupling regime. Thus, we conclude that the new model discussed here is a natural generalization to $d_{x^2-y^2}$ superconductivity of the attractive Hubbard model. The new model is based on the phenomenology of the high- T_c cuprates, which is dominated near the half-filling by antiferromagnetic fluctuations. Phenomenological studies of the influence of impurities, external fields, and other probes on the $d_{x^2-y^2}$ superconductivity would become more accurate if model (1) replaces the $t - U - V$ model.

The authors are sincerely grateful to Prof. Yurii Gorobets, and Prof. Ernst Pashitskii for the fruitful discussions, comments, and continuous support of the research.

The work was sponsored by the Institute of Magnetism of the National Academy of Sciences of Ukraine and the National Technical University of Ukraine “KPI” of the Ministry of Education and Science of Ukraine.

1. A.J. Leggett, in *Modern Trends in the Theory of Condensed Matter*, edited by A. Pekalski and R. Przystawa, (Springer, Berlin, 1980).
2. R.T. Scalettar *et al.*, Phys. Rev. Lett. **62**, 1407 (1989); A. Moreo and D. Scalapino, Phys. Rev. Lett. **66**, 946 (1991); M. Randeria, N. Trivedi, A. Moreo, and R.T. Scalettar, Phys. Rev. Lett. **69**, 2001 (1992).
3. D.J. Scalapino, Phys. Rep. **250**, 331 (1995).
4. N.M. Plakida, *High-Temperature Superconductivity: Experiment and Theory* (Springer, Berlin, 1995).
5. C.A.R. Sá de Melo, M. Randeria, and J.R. Engelbrecht, Phys. Rev. Lett. **71**, 3202 (1993).
6. W. Li *et al.*, arXiv:1203.2581 (2012); A. Kordyuk, Visnyk NAN Ukrainy, No. 9, 46 (2012).
7. R. Micnas *et al.*, Rev. Mod. Phys. **62**, 113 (1990); E. Dagotto *et al.*, Phys. Rev. B **49**, 3548 (1994).
8. S. Haas *et al.*, Phys. Rev. B **51**, 5989 (1995).
9. A. Sboychakov *et al.*, Phys. Rev. B **77**, 224504 (2008).

10. E. Dagotto, Rev. Mod. Phys. **66**, 763 (1994).
11. Another possible model of d -wave SC can be obtained by selecting a pair-pair interaction which is separable in the momentum-space. In particular, $\sum_{\mathbf{k}, \mathbf{k}'} c_{\mathbf{k}\uparrow}^\dagger c_{-\mathbf{k}\downarrow} c_{\mathbf{k}'\uparrow}^\dagger c_{-\mathbf{k}'\downarrow}$ ($\cos k_x - \cos k_y$)($\cos k'_x - \cos k'_y$) would be enough to produce d -wave SC. The study of this model will be addressed in the near future publications. See also R. Gonczarek, M. Krzyzosiak, and A. Gonczarek, Eur. Phys. J. B **61**, 299 (2008).
12. E.A. Pashitskii and V.I. Pentegov, Low Temp. Phys. **34**, 113, (2008).
13. M.M. Korshunov *et al.*, JETP **99**, 559 (2004).
14. Strong numerical indications of d -wave SC have been found before in the related models, in particular, in the $t - J$ model (see, e.g., E. Dagotto and J. Riera, Phys. Rev. Lett. **70**, 682 (1993); Y. Ohta *et al.*, Phys. Rev. Lett. **73**, 324 (1994); A. Nazarenko *et al.*, Phys. Rev. B **54**, R768 (1996)).
15. E. Dagotto, A. Nazarenko, and A. Moreo, Phys. Rev. Lett. **74**, 728 (1994).
16. E. Dagotto, A. Nazarenko, and M. Boninsegni, Phys. Rev. Lett. **73**, 310 (1995); A. Nazarenko and E. Dagotto, Phys. Rev. B **54**, 13158 (1996).
17. C. Dürr *et al.*, Phys. Rev. B **63**, 014505 (2001).
18. D. Duffy *et al.*, Phys. Rev. B **56**, 5597 (1997).
19. P. Monthoux and D. Pines, Phys. Rev. Lett. **69**, 961 (1992).
20. D.Z. Liu, K. Levin, and J. Maly, Phys. Rev. B **51**, 8680 (1995).
21. S. Ovchinnikov *et al.*, Phys. Sol. State **53**, 242 (2011).
22. P. Monthoux and D. Scalapino, Phys. Rev. Lett. **72**, 1874 (1994).
23. Our numerical calculations reveal that keeping only the one-loop diagram in the effective potential produces a spurious s -wave condensate.
24. Yu.G. Pogorelov, M.C. Santos, V.M. Loktev, Low Temp. Phys., **37**, 633 (2011); Yu.G. Pogorelov, V.M. Loktev, Phys. Rev. B **69**, 214508 (2004).
25. A.A. Abrikosov, L.P. Gorkov, and I.E. Dzyaloshinsky, *Methods of Quantum Field Theory in Statistical Physics* (Dover, New York, 1975).
26. For a uniform system, the tadpole diagram including the fermionic Green's function, which closes on itself, leads to the renormalization of the chemical potential for a short-

range bare interaction between fermions. Therefore, it should not be included in the self-consistent scheme, since the chemical potential itself is calculated self-consistently from the conservation of the number of particles, which absorbs all constant shifts (including those from the tadpole family of diagrams). In the case of a long-range potential like the Coulomb one, the tadpole diagram leads to the divergency of the ground-state energy, but this is eliminated by the electroneutrality of the system of charged fermions immersed in the uniform opposite ambient charge, which can be easily demonstrated on the Coulomb interaction with the screening having the following Fourier transform in the \mathbf{k} -space: $V(\mathbf{k}) = \frac{4\pi e^2}{\mathbf{k}^2 + \kappa^2}$, where κ is the reciprocal screening length. The one-bubble tadpole diagram is proportional to: $V(\mathbf{k} = 0)n_e$, n_e is the concentration of electrons. If $\kappa \neq 0$, it reduces to the constant $4\pi e^2 n_e / \kappa^2$. If $\kappa = 0$, its contribution diverges, and one needs the uniform positive background with the same charge to immerse the system of electrons to cancel both divergencies of opposite sign.

Received 25.02.13

I.В. Бар'яхтар, О.Б. Назаренко

МОДЕЛЬ ДЛЯ $d_{x^2-y^2}$ НАДПРОВІДНОСТІ В СИЛЬНОКОРЕЛЬОВАНИЙ ФЕРМІОННІЙ СИСТЕМІ

Резюме

Пропонується двовимірна ефективна ферміонна модель з притяганням до найближчих сусідів, що ґрунтується на відомій феноменології ВТНП і існуючих чисельних розрахунках у моделі $t - J$. Чисельні розрахунки показують, що модель має $d_{x^2-y^2}$ надпровідність в основному стані при низьких ферміонних концентраціях. Ми стверджуємо, що ця модель відображає важливу фізику $d_{x^2-y^2}$ надпровідних кореляцій, знайдених раніше в $t - J$ моделі в підході точної діагоналізації. У рамках самоузгодженого наближення хаотичних фаз обчислено залежності критичної температури від концентрації і константи зв'язку. Досліджується також вплив домішок на наші результати і показано, що при обліку ефектів запізнювання зниження надпровідності незначне, на відміну від наближення Хартрі-Фока.